Letter

Searching for cosmic string induced stochastic gravitational wave background with the Parkes Pulsar Timing Array

Ligong Bian,[1,2,*] Jing Shu,[3,2,4,5,6,7,†] Bo Wang,[7] Qiang Yuan,[8,9,‡] and Junchao Zong[10,4]

[1]*Department of Physics and Chongqing Key Laboratory for Strongly Coupled Physics, Chongqing University, Chongqing 401331, China*
[2]*Center for High Energy Physics, Peking University, Beijing 100871, China*
[3]*School of Physics and State Key Laboratory of Nuclear Physics and Technology, Peking University, Beijing 100871, China*
[4]*CAS Key Laboratory of Theoretical Physics, Institute of Theoretical Physics, Chinese Academy of Sciences, Beijing 100190, China*
[5]*School of Physical Sciences, University of Chinese Academy of Sciences, Beijing 100049, China*
[6]*School of Fundamental Physics and Mathematical Sciences, Hangzhou Institute for Advanced Study, University of Chinese Academy of Sciences, Hangzhou 310024, China*
[7]*International Centre for Theoretical Physics Asia-Pacific, University of Chinese Academy of Sciences, 100190 Beijing, China*
[8]*Key Laboratory of Dark Matter and Space Astronomy, Purple Mountain Observatory, Chinese Academy of Sciences, Nanjing 210023, China*
[9]*School of Astronomy and Space Science, University of Science and Technology of China, Hefei 230026, China*
[10]*Department of Physics, Nanjing University, Nanjing 210093, China*

(Received 20 May 2022; accepted 11 October 2022; published 14 November 2022)

We search for stochastic gravitational wave background emitted from cosmic strings using the Parkes Pulsar Timing Array data over 15 years. While the common power-law excess revealed by several pulsar timing array experiments might be accounted for by the gravitational wave background from cosmic strings, the lack of the characteristic Hellings-Downs correlation cannot establish its physical origin yet. The constraints on the cosmic string model parameters are thus derived with the conservative assumption that the common power-law excess is due to unknown background. Two representative cosmic string models with different loop distribution functions are considered. We obtain constraints on the dimensionless string tension parameter $G\mu < 10^{-11}$–10^{-10}, which is more stringent by two orders of magnitude than that obtained by the high-frequency LIGO-Virgo experiment for one model, and less stringent for the other. The results provide the chance to test the grand unified theories, with the spontaneous symmetry breaking scale of $U(1)$ being two-to-three orders of magnitude below 10^{16} GeV. The pulsar timing array experiments are thus entirely complementary to the LIGO-Virgo experiment in probing the cosmic strings and the underlying beyond standard model physics in the early Universe.

DOI: 10.1103/PhysRevD.106.L101301

I. INTRODUCTION

Cosmic strings (CSs) are one-dimensional topological defects formed during phase transitions where symmetry gets broken spontaneously [1,2]. The Nambu-Goto action can describe the CS dynamics for thin and local strings with no internal structures. In this situation, infinite strings can reach the scaling regime [3–5] and go to loops through the intercommutation of intersecting string segments [6]. They form small loops which oscillate and emit gravitational wave (GW) bursts by the structures of Cusps and Kinks [7,8]. The superposition of uncorrelated GW bursts from many CSs forms a stochastic gravitational wave background (SGWB). In the Nambu-Goto string scenario, the SGWB is characterized by the loop number density, and the string tension (μ) [9]. The dimensionless parameter $G\mu$ (G is the Newtonian constant) that represents the gravitational interaction strength of strings is tightly connected to the symmetry breaking scale η as $G\mu \sim (\eta/M_{\rm Mpl})^2$.

*lgbycl@cqu.edu.cn
†jshu@pku.edu.cn
‡yuanq@pmo.ac.cn

Published by the American Physical Society under the terms of the Creative Commons Attribution 4.0 International license. Further distribution of this work must maintain attribution to the author(s) and the published article's title, journal citation, and DOI. Funded by SCOAP³.

Usually η is a very high scale since CSs are generally predicted in grand unified theories (GUT) or supersymmetry breaking [10,11]. Therefore, the detection of SGWB from CSs provide an intriguing way to access the beyond-standard-model physics close to the GUT scale that are inaccessible by high-energy colliders [19–22], such as leptogenesis and the type-I seesaw scale [23].

The gravitational waves spectra from CSs span a wide frequency range characterized by a plateau in the high-frequency region. The SGWB from CSs is one of the most promising target of LIGO-Virgo [24,25], Laser Interferometer Space Antenna (LISA) [26], and pulsar timing arrays (PTA) [27–29]. Recently, both LIGO-Virgo and PTA experiments made great progress on the search of GWs from CSs. The LIGO-Virgo group place stringent constraints on the GW bursts and the SGWB from CSs in the high-frequency window [24]. In the nanohertz range, the PPTA collaboration searched for the bursts from cusps of the CS, and placed effective constraints on the string tension [27]. Several PTAs reported the detection of a mysterious common red process [30–35], which may be explained as SGWB from various sources including CSs [34,36–38]. However, the GW interpretation of the common red process is still suspicious due to the lack of the characteristic Hellings-Downs (HD) correlation in the data [39], which describes the correlation of signals as a function of angles between pulsar pairs observed at the Earth and is regarded as the smoking gun for the gravitational wave detection because of its unique quadruple feature. LIGO-Virgo experiments are more sensitive to the high frequency range of the SGWB spectra of CSs corresponding to GWs contribution from the radiations era. Meanwhile, the PTA experiments are more sensitive to the nanohertz range. They can play an essential role in searching for SGWBs emitted from CS loops formed both in the radiation dominated era but surviving until the matter dominated era and directly in the matter dominated era. In this work we search for SGWB signals generated from CSs utilizing the Parkes Pulsar Timing Array (PPTA) data. We consider two representative SGWB models of CSs with two different loop distribution functions and derive the constraints on the dimensionless $G\mu$ parameter of CS. The results can be translated into the constraints on the symmetry breaking scale η to probe the high scale physics, such as GUT.

II. SGWB SPECTRA FOR COSMIC STRING NETWORKS

The SGWB from cosmic string networks comes from the uncorrelated superpositions of GW bursts of three contributions: cusps, kinks, and kink-kink collision. The SGWB spectrum emitted from cosmic strings is given by

$$\Omega_{\rm GW}(t_0,f)=\frac{f}{\rho_c}\frac{d\rho_{\rm GW}}{df}(t_0,f), \tag{1}$$

where $\rho_c=\frac{3H_0^2}{8\pi G}$ is the critical energy density of the universe, $\frac{d\rho_{\rm GW}}{df}(t_0,f)$ is the GWs energy density per unit frequency today. Considering different modes of loops oscillation (n), we have

$$\frac{d\rho_{\rm GW}}{df}(t_0,f)=G\mu^2\sum_n C_n(f)P_n, \tag{2}$$

where the $C_n(f)$ is a function of loop distributions depending on the cosmological background. To account for all contributions from cusps, kinks, and kink-kink collisions, we adopt the P_n from numerical simulations [40]. Analytically, $P_n=\frac{\Gamma}{\zeta(q)}n^{-q}$, $\Gamma\approx 50$ and $\zeta(q)$ is the Riemann zeta function with $q=4/3$, $5/3$, and 2 representing for cusps, kinks, and kink-kink collisions, respectively.

We first consider the SGWB from CSs with the loop production functions for nonself-intersecting loops being obtained directly from CS networks simulation in radiation and matter dominated era by Blanco-Pillado, Olum, Shlaer [41,42] (hereafter denoted as BOS model, which is dubbed as model A by LIGO-Virgo group in Ref. [24]). In this model, one needs to take into account contributions from the radiation dominated era and the matter dominated era with the loop number density $n(l,t)$ given in the Supplemental Material [43]. For the SGWB contributions from the radiation era, one has

$$C_n(f)=\frac{2n}{f^2}\int_{z_{\rm eq}}^{z_{\rm cut}}\frac{dz}{H_0\sqrt{\Omega_r}(1+z)^8}n_r(l,t), \tag{3}$$

where $z_{\rm eq}$ is the redshift in the radiation-matter equality and $z_{\rm cut}$ is the cutoff redshift. The subscript r here denotes radiation dominated era, similarly, in the following rm is for the case where loops are formed in radiation dominated era but survive past to matter dominated era and m for the case of matter dominated era. We note that here the $n_r(l,t)$ is the loop distribution function rather than the oscillation mode n before the integration. The SGWB contributions from matter dominated era constitute two parts: loops that survive to matter dominated era and loops formed in matter dominated era. The C_n takes the form of

$$C_n(f)=\frac{2n}{f^2}\int_0^{z_{\rm eq}}\frac{dz}{H_0\sqrt{\Omega_m}(1+z)^{15/2}}n_i(l,t), \tag{4}$$

with i being rm and m for these two cases, respectively. In this work, we adopt the Hubble constant as $H_0=67.8\ {\rm km\,s^{-1}\,Mpc^{-1}}$, the radiation density as $\Omega_r=9.1476\times10^{-5}$, and the matter density as $\Omega_m=0.308$ [44].

Following the same procedure, we can calculate the SGWB spectrum with loop distribution functions being derived analytically by Lorenz, Ringeval, and Sakellariadou [45] (denoted as LRS, which is dubbed as model B by LIGO-Virgo group in Ref. [24]), where the

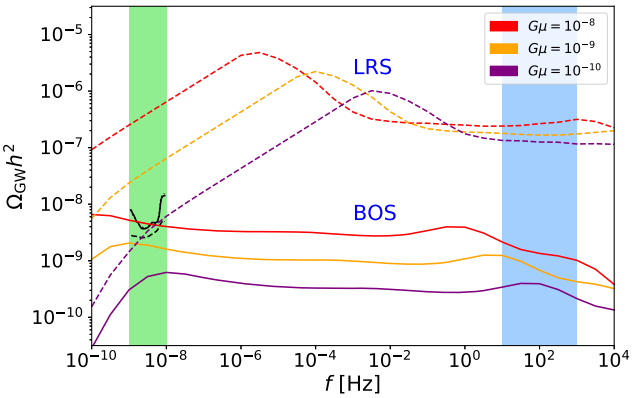

FIG. 1. Expected spectra of SGWB from CS for the BOS (LRS) model with $G\mu = 10^{-8}$, 10^{-9}, and 10^{-10}, which are indicated by red, orange, and purple solid (dashed) lines. The solid and dashed black lines represent the 95% C.L. upper limits for free spectrum assumption derived from the PPTA data for different hypotheses (H2/H3 and H4 in Tables I and II, respectively). The sensitive frequency regions of PTA and LIGO-Virgo are denoted by green and blue shaded bands.

distribution of nonself-intersecting scaling loops are extracted from simulations [46].

Figure 1 shows the total SGWB spectra of the CS-induced SGWB for the BOS and LRS models, for a few values of $G\mu$. It shows that the BOS model predicts relatively flat spectra (solid lines) and hence the PTA experiment is more suitable to probe it. On the other hand, the LRS model predicts stronger spectra at high frequencies (dashed lines) which is more optimal for the high-frequency GW experiment such as LIGO-Virgo. Also shown in Fig. 1 are the upper limits of the free-spectrum SGWB derived from the PPTA data [47]. We find that the CS models with $G\mu$ of $10^{-8} \sim 10^{-10}$ are severely constrained by the PPTA data. The magnitude of the SGWB spectra for the LRS model is much higher than that of the BOS model at high frequencies due to the larger number of small loops in the loop distribution function dominant in such frequency range.

III. DATA ANALYSIS

The dataset we used in this work is the second data release (DR2) of the PPTA [48], which is available in the CSIRO pulsar data archive [49]. Searches for SGWBs and other fundamental physics problems using these data (or the subsets) were also carried out [31,47,50–52]. In PTA, to search for such an SGWB signal from CS is to find spatially correlated time residuals among time-of-arrivals (ToA) of different pulsars. The residuals are composed of deterministic timing models, noises, and the hypothetical signal (SGWB from CS here). We use the `TEMPO2` tool [53,54] to fit the timing models of pulsars, the `ENTERPRISE` [55] and the `ENTERPRISE_EXTENSIONS` [56] to model the noises, and `PTMCMCSampler` [57] to do the Bayesian analysis. The noise model is based on single pulsar analyses of Ref. [58]. Briefly speaking, the stochastic noises mainly include two parts, the white noise and red noise. The white noise may come from the radio frequency interference, pulse profile changes or instrumental artifacts. We use three parameters, `EFAC` (Error FACtor), `EQUAD` (Error added in QUADrature) and `ECORR` (Error of CORRelation between ToAs in a single epoch), to account for white noise which cannot be subtracted by fitting the timing model. As usually done [51,52], we fix the white noise parameters as their maximum likelihood values from the single pulsar analyses in the Bayesian analysis. The red noises are mainly caused by the irregularities of the pulsar spin (spin noise) and the dispersion measure of photons when traveling through the interstellar medium (DM noise). For some pulsars there are band noise for ToAs of a certain photon frequency band and chromatic noise which correlates between different photon frequencies. All the red noises are modeled as power-law forms with amplitude A and slope γ. Several analyses revealed that there is a common power-law (CPL) process in the pulsar ToAs, whose nature is still in debate [30–33]. In this work we will test different assumptions on the CPL, as either the SGWB signal from CS (see also [36,37]) or an unknown background. The solar system ephemeris uncertainties are modeled with a 11-parameter model `BayesEphem` implemented in `ENTERPRISE`, including perturbations in masses of major planets, the drift rate of the Earth-Moon barycenter orbit, and the perturbations of the Earth's orbit from Jupiter's average orbital elements described by 6 parameters [59]. We summarize the noise and signal parameters together with their priors adopted in the Bayesian analysis in Table S1 in the Supplemental Material [43].

IV. RESULTS

To address the significance of the CS-induced SGWB signal in the data, we test the Bayes factor (BF) of the "signal hypothesis" against the null hypothesis, following the Savage-Dickey formula [60]

$$\mathrm{BF}_{10} = \frac{P_1(\boldsymbol{D})}{P_0(\boldsymbol{D})} = \frac{P(\boldsymbol{\phi} = \boldsymbol{\phi}_0)}{P(\boldsymbol{\phi} = \boldsymbol{\phi}_0|\boldsymbol{D})}, \tag{5}$$

where BF_{10} means the BF of hypothesis H1 against H0, $\boldsymbol{D}$ is the observational data, $\boldsymbol{\phi}$ is the parameters of the signal model, and $\boldsymbol{\phi_0}$ is the parameters of the null hypothesis which is a subset of $\boldsymbol{\phi}$. P_0 and P_1 are the evidence of the noise and signal hypotheses. The BF_{10} is equivalent to the ratio of the prior to the posterior probabilities of the null hypothesis.

The null hypothesis (H0) corresponds to the model with only the pulsar timing model and noise. For hypothesis H1, we assume an additional CPL process in the model. The CS model with the HD correlation included in substitution of the CPL process is labelled as H2. In addition, in H3 and H4 we

TABLE I. Hypotheses, Bayes factors, and estimated model parameters for the BOS model.

Hypothesis	Pulsar Noise	CPL Process	HD process CS spectrum	Bayes Factors	Parameter Estimation (68% C.L.)	
					$\log_{10} G\mu$	$\log_{10} A_{\rm CPL}, \gamma_{\rm CPL}$
H0:Pulsar Noise	✓					
H1:CPL	✓	✓		$10^{3.2}$ (/H0)		$-14.48^{+0.62}_{-0.64}, 3.34^{+1.37}_{-1.53}$
H2:CS	✓		✓ (full HD)	$10^{3.1}$ (/H0)	$-10.38^{+0.21}_{-0.21}$	
H3:CS1	✓	✓	✓ (full HD)	1.96 (/H1)	<-10.02 (95% C.L.)	$-15.58^{+1.21}_{-1.64}, 3.11^{+1.95}_{-2.02}$
H4:CS2	✓	✓	✓ (no-auto HD)	0.60 (/H1)	<-10.54 (95% C.L.)	$-14.61^{+0.58}_{-0.59}, 3.63^{+1.24}_{-1.40}$

TABLE II. Hypotheses, Bayes factors, and estimated model parameters for the LRS model.

Hypothesis	Pulsar Noise	CPL Process	HD process CS spectrum	Bayes Factors	Parameter Estimation (68% C.L.)	
					$\log_{10} G\mu$	$\log_{10} A_{\rm CPL}, \gamma_{\rm CPL}$
H0:Pulsar Noise	✓					
H1:CPL	✓	✓		$10^{3.2}$ (/H0)		$-14.48^{+0.62}_{-0.64}, 3.34^{+1.37}_{-1.53}$
H2:CS	✓		✓ (full HD)	$10^{3.3}$ (/H0)	$-10.89^{+0.14}_{-0.17}$	
H3:CS1	✓	✓	✓ (full HD)	1.62 (/H1)	<-10.64 (95% C.L.)	$-15.44^{+1.18}_{-1.74}, 3.08^{+1.94}_{-1.99}$
H4:CS2	✓	✓	✓ (no-auto HD)	0.55 (/H1)	<-11.04 (95% C.L.)	$-14.57^{+0.58}_{-0.59}, 3.54^{+1.24}_{-1.41}$

consider simultaneously the CPL process as an unknown systematics and the CS contribution, in which the autocorrelation of a pulsar's own ToAs is not subtracted (H3) and subtracted (H4), respectively. The results of the fittings for different hypotheses are summarized in Tables I and II.

For hypothesis H1, a clear CPL signal with a BF of $10^{3.2}$ is revealed in the data, consistent with previous studies [30–33]. The posterior distributions of the CPL model parameters are shown in Fig. S1 in the Supplemental Material [43]. Similar signal with comparable BF value is found if we assume a CS-induced SGWB component in the model rather than the CPL (H2). Fitting results of the CS parameter $\log_{10} G\mu$ are -10.38 ± 0.21 and $-10.89^{+0.14}_{-0.17}$ for the BOS and LRS model, with 1σ error bars presented. The corresponding parameter values are consistent with that employed to account for the NANOGrav data, but with different model assumptions [36]. Since the nature of the CPL process is unclear, and particularly the characteristic HD correlation of GWs is still lacking, we also test the hypotheses that treating the CPL as an unknown background. The resulting BF of hypotheses H3 or H4 against H1 is close to 1 which means that the evidence of the CS is not significant in case of a CPL background. We therefore derive the 95% credible level (C.L.) upper limits on $\log_{10} G\mu$, as given in Tables I and II. The posterior distributions of the CPL and CS parameters for H4 are shown in Fig. 2. More results of the analysis based on different hypotheses can be found in Figs. S2–S3 in the Supplemental Material [43]. Additional tests assuming that the CPL has an astrophysical origin from the supermassive binary black hole (SMBBH) give similar conclusion (see the Supplemental Material [43]).

Our results can be compared with those obtained by the LIGO-Virgo observations of high-frequency GWs [24], which is displayed in Fig. 3. We also show the bound from the cosmic microwave background (CMB), while the less stronger limit from big bang nucleosynthesis (BBN) is too weak to be shown in the figure [24,61]. The LIGO-Virgo

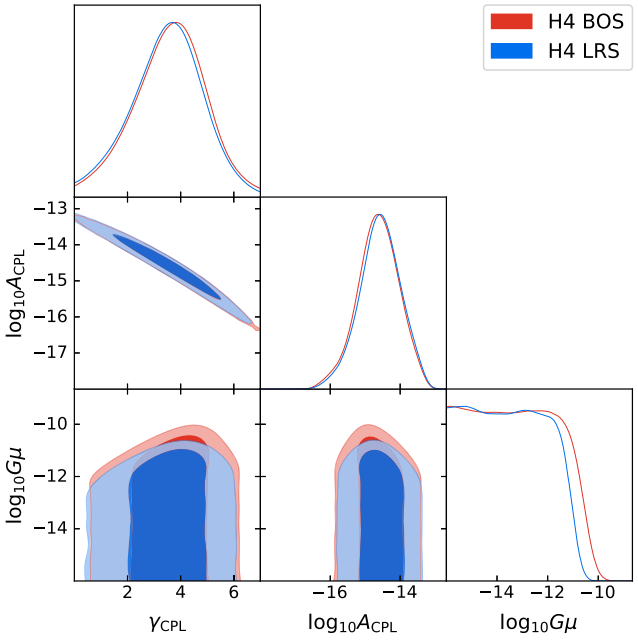

FIG. 2. Posteriors distribution of $\log_{10} G\mu$ and the CPL parameters of BOS (red) and LRS (blue) models assuming a no-auto HD correlation. The 68% C.L. and 95% C.L. ranges are presented in light and dark colors.

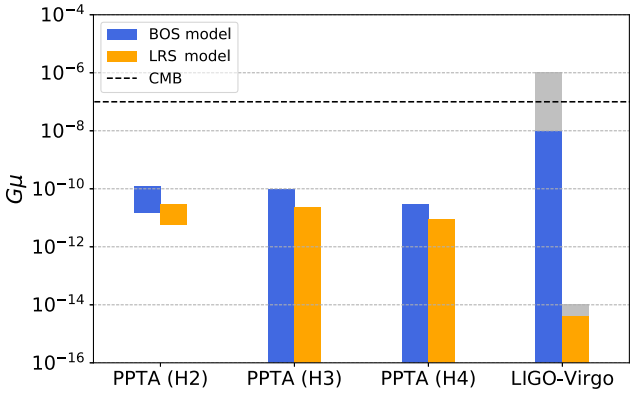

FIG. 3. Constraints on $G\mu$ at the 95% C.L. from the PPTA data for different hypotheses, compared with those obtained by LIGO-Virgo experiment [24]. Silver boxes represent the ranges reported in the LIGO-Virgo analysis. The limit from cosmic microwave background (CMB) is also reported by the black dashed line [61].

upper limits of $G\mu$ are 10^{-8}–10^{-6} and $(4.0-6.3)\times 10^{-15}$ for the BOS and LRS model (model A and B in [24]), respectively. Compared with LIGO-Virgo results, the PPTA upper limits on $\log_{10} G\mu$ improve by more than two orders of magnitude for the BOS model. For the LRS model, the LIGO-Virgo result is more stringent because the SGWB spectrum is steeper. The PTA experiment is thus very complementary to the LIGO-Virgo experiment for the searches of CS-induced SGWB.

V. CONCLUSION

The very precise timing measurements of pulsars provide a powerful tool to probe the fundamental new physics process occurred in the early Universe. In this work we use more than 15 years of observations of 26 millisecond pulsars by the PPTA experiment to search for SGWB from CS networks. We show that the CPL process revealed by several PTAs recently can be explained by the CS-induced SGWB signal with $\log_{10} G\mu \sim -10.38$ and -10.89 for the two typical classes of CS models, the BOS and LRS models. While the LRS model explanation would be excluded by the LIGO-Virgo observations at high frequencies, the BOS model explanation is consistent with the LIGO-Virgo data [24]. As a conservative alternative, we also assume the CPL as a background component and turn to set limits on the CS model parameters. The PPTA upper limits on $\log_{10} G\mu$ reach about $-10 \sim -11$, depending on the CS models and the analysis methods. These constraints correspond to the symmetry breaking scale $\eta \sim 10^{13}$–10^{14} GeV, that challenge the grand unification theories below the GUT scale already. For the BOS model, the PPTA limits are more stringent than those from LIGO-Virgo, and for the LRS model the LIGO-Virgo experiment is more sensitive. This is due to the fact that, in the LRS model, more small loops are contained in the loop distribution functions that control the behaviors of the SGWB spectra from CS networks in high frequency range. We expect that continuous accumulation of more precise data by PTAs around the world in the near future will critically test the CS models and more generally, a class of GUTs admitting the U(1) symmetry breaking in the early Universe.

Superstrings that are generally predicted in string theories can evolve as CS networks [62–67] with 1 to 3 orders of magnitude lower intercommutation probabilities. That leads to an increase of the loop number density and hence the amplitude of the SGWB, thus a tighter limit on the $G\mu$ can be obtained. For the study with NANOGrav 12.5-yr data we refer to Ref. [34].

ACKNOWLEDGMENTS

This work uses the public data from the Parkes Pulsar Timing Array. We thank Huai-Ke Guo and Yue Zhao for useful discussions, and appreciate Xiao Xue for the help on the data analysis in the early stage of this work. L. B. is supported by the National Key Research and Development Program of China under Grant No. 2021YFC2203004, the National Natural Science Foundation of China (NSFC) under Grants No. 12075041 and No. 12047564, the Fundamental Research Funds for the Central Universities of China under Grants No. 2021CDJQY-011 and No. 2020CDJQY-Z003, and Chongqing Natural Science Foundation under Grant No. cstc2020jcyj-msxmX0814. J. S. is supported by Peking University under startup Grant No. 7101302974 and the NSFC under Grants No. 12025507, No. 11690022, and No. 11947302, by the Strategic Priority Research Program and Key Research Program of Frontier Science of the Chinese Academy of Sciences (CAS) under Grants No. XDB21010200, No. XDB23010000, No. XDPB15, and No. ZDBS-LY-7003, and by the CAS Project for Young Scientists in Basic Research under Grant No. YSBR-006. Q. Y. is supported by the Program for Innovative Talents and Entrepreneur in Jiangsu and the Key Research Program of CAS under Grant No. XDPB15.

Note added.—We note that a similar study on the search for CS-induced SGWB using the PPTA data appeared on arXiv at the same time of this work [68]. The models used of these two works are slightly different, they consider the cosmic superstrings and use an extended BOS model with an additional parameter p, represents the reconnection probability of strings [40]. Their model would be back to the BOS model as this work when $p = 1$, and the results are also consistent with ours.

[1] T. W. B. Kibble, J. Phys. A **9**, 1387 (1976).
[2] M. B. Hindmarsh and T. W. B. Kibble, Rep. Prog. Phys. **58**, 477 (1995).
[3] D. P. Bennett and F. R. Bouchet, Phys. Rev. Lett. **60**, 257 (1988).
[4] B. Allen and E. P. S. Shellard, Phys. Rev. Lett. **64**, 119 (1990).
[5] M. Sakellariadou and A. Vilenkin, Phys. Rev. D **42**, 349 (1990).
[6] T. Vachaspati and A. Vilenkin, Phys. Rev. D **30**, 2036 (1984).
[7] T. Damour and A. Vilenkin, Phys. Rev. D **64**, 064008 (2001).
[8] T. Damour and A. Vilenkin, Phys. Rev. Lett. **85**, 3761 (2000).
[9] A. Vilenkin and E. P. S. Shellard, *Cosmic Strings and Other Topological Defects* (Cambridge University Press, Cambridge, England, 2000), ISBN 978-0-521-65476-0.
[10] Y. Cui, S. P. Martin, D. E. Morrissey, and J. D. Wells, Phys. Rev. D **77**, 043528 (2008).
[11] We note that, for global strings which are motivated for axion or axionlike particles at GUT scale [12], CSs mostly decay through particle radiation rather than GW radiations [13]. Recent large field simulations of local strings suggest that particle or GW radiation dominates the CS decay mode for small or large loops [14]. The exact portion of particle radiation and GW radiation emitted by CS networks may be settled down by simulations in the near future [14–18].
[12] Q. Yang, H. Yu, and H. Di, Phys. Dark Universe **26**, 100407 (2019).
[13] A. Saurabh, T. Vachaspati, and L. Pogosian, Phys. Rev. D **101**, 083522 (2020).
[14] D. Matsunami, L. Pogosian, A. Saurabh, and T. Vachaspati, Phys. Rev. Lett. **122**, 201301 (2019).
[15] M. Hindmarsh, J. Lizarraga, J. Urrestilla, D. Daverio, and M. Kunz, Phys. Rev. D **96**, 023525 (2017).
[16] M. Hindmarsh, J. Lizarraga, A. Urio, and J. Urrestilla, Phys. Rev. D **104**, 043519 (2021).
[17] G. Vincent, N. D. Antunes, and M. Hindmarsh, Phys. Rev. Lett. **80**, 2277 (1998).
[18] D. Daverio, M. Hindmarsh, M. Kunz, J. Lizarraga, and J. Urrestilla, Phys. Rev. D **93**, 085014 (2016); **95**, 049903(E) (2017).
[19] S. F. King, S. Pascoli, J. Turner, and Y.-L. Zhou, J. High Energy Phys. 10 (2021) 225.
[20] S. F. King, S. Pascoli, J. Turner, and Y.-L. Zhou, Phys. Rev. Lett. **126**, 021802 (2021).
[21] W. Buchmuller, V. Domcke, H. Murayama, and K. Schmitz, Phys. Lett. B **809**, 135764 (2020).
[22] R. Caldwell *et al.*, arXiv:2203.07972.
[23] J. A. Dror, T. Hiramatsu, K. Kohri, H. Murayama, and G. White, Phys. Rev. Lett. **124**, 041804 (2020).
[24] R. Abbott *et al.* (LIGO Scientific, Virgo, and KAGRA Collaborations), Phys. Rev. Lett. **126**, 241102 (2021).
[25] B. P. Abbott *et al.* (LIGO Scientific and Virgo Collaborations), Phys. Rev. D **97**, 102002 (2018).
[26] P. Auclair *et al.*, J. Cosmol. Astropart. Phys. 04 (2020) 034.
[27] N. Yonemaru *et al.*, Mon. Not. R. Astron. Soc. **501**, 701 (2021).
[28] S. A. Sanidas, R. A. Battye, and B. W. Stappers, Phys. Rev. D **85**, 122003 (2012).
[29] P. G. Auclair, J. Cosmol. Astropart. Phys. 11 (2020) 050.
[30] Z. Arzoumanian *et al.* (NANOGrav Collaboration), Astrophys. J. Lett. **905**, L34 (2020).
[31] B. Goncharov *et al.*, Astrophys. J. Lett. **917**, L19 (2021).
[32] S. Chen *et al.*, Mon. Not. R. Astron. Soc. **508**, 4970 (2021).
[33] J. Antoniadis *et al.*, Mon. Not. R. Astron. Soc. **510**, 4873 (2022).
[34] J. J. Blanco-Pillado, K. D. Olum, and J. M. Wachter, Phys. Rev. D **103**, 103512 (2021).
[35] Z.-C. Chen, Y.-M. Wu, and Q.-G. Huang, Commun. Theor. Phys. **74**, 105402 (2022).
[36] J. Ellis and M. Lewicki, Phys. Rev. Lett. **126**, 041304 (2021).
[37] L. Bian, R.-G. Cai, J. Liu, X.-Y. Yang, and R. Zhou, Phys. Rev. D **103**, L081301 (2021).
[38] S. Blasi, V. Brdar, and K. Schmitz, Phys. Rev. Lett. **126**, 041305 (2021).
[39] R. W. Hellings and G. S. Downs, Astrophys. J. Lett. **265**, L39 (1983).
[40] J. J. Blanco-Pillado and K. D. Olum, Phys. Rev. D **96**, 104046 (2017).
[41] J. J. Blanco-Pillado, K. D. Olum, and B. Shlaer, Phys. Rev. D **89**, 023512 (2014).
[42] J. J. Blanco-Pillado, K. D. Olum, and B. Shlaer, Phys. Rev. D **83**, 083514 (2011).
[43] Please see Supplemental Material at http://link.aps.org/supplemental/10.1103/PhysRevD.106.L101301 for details of the loop distribution of the two cosmic string models, the prior distribution of the PTA model parameters, posterior distributions of other hypotheses in the tables and searching results for an interpretation for the common power-law excess from the SMBBH.
[44] N. Aghanim *et al.* (Planck), Astron. Astrophys. **641**, A6 (2020); **652**, C4(E) (2021).
[45] L. Lorenz, C. Ringeval, and M. Sakellariadou, J. Cosmol. Astropart. Phys. 10 (2010) 003.
[46] C. Ringeval, M. Sakellariadou, and F. Bouchet, J. Cosmol. Astropart. Phys. 02 (2007) 023.
[47] X. Xue *et al.*, Phys. Rev. Lett. **127**, 251303 (2021).
[48] M. Kerr *et al.*, Pub. Astron. Soc. Aust. **37**, e020 (2020).
[49] 10.4225/08/5afff8174e9b3.
[50] R. M. Shannon *et al.*, Science **349**, 1522 (2015).
[51] N. K. Porayko *et al.*, Phys. Rev. D **98**, 102002 (2018).
[52] X. Xue *et al.* (PPTA Collaboration), Phys. Rev. Res. **4**, L012022 (2022).
[53] G. Hobbs, R. Edwards, and R. Manchester, Mon. Not. R. Astron. Soc. **369**, 655 (2006).
[54] R. T. Edwards, G. B. Hobbs, and R. N. Manchester, Mon. Not. R. Astron. Soc. **372**, 1549 (2006).
[55] https://github.com/nanograv/enterprise.
[56] https://github.com/nanograv/enterprise_extensions.
[57] J. Ellis and R. van Haasteren, jellis18/ptmcmcsampler: Official Release, 10.5281/zenodo.1037579 (2017).
[58] B. Goncharov *et al.*, Mon. Not. R. Astron. Soc. **502**, 478 (2021).
[59] Z. Arzoumanian *et al.* (NANOGRAV Collaboration), Astrophys. J. **859**, 47 (2018).
[60] J. M. Dickey, Ann. Math. Stat. **42**, 204 (1971).

[61] P. A. R. Ade *et al.* (Planck Collaboration), Astron. Astrophys. **571**, A25 (2014).
[62] M. G. Jackson, N. T. Jones, and J. Polchinski, J. High Energy Phys. 10 (2005) 013.
[63] E. J. Copeland, R. C. Myers, and J. Polchinski, J. High Energy Phys. 06 (2004) 013.
[64] N. T. Jones, H. Stoica, and S. H. H. Tye, Phys. Lett. B **563**, 6 (2003).
[65] G. Dvali and A. Vilenkin, J. Cosmol. Astropart. Phys. 03 (2004) 010.
[66] S. Sarangi and S. H. H. Tye, Phys. Lett. B **536**, 185 (2002).
[67] N. T. Jones, H. Stoica, and S. H. H. Tye, J. High Energy Phys. 07 (2002) 051.
[68] Z.-C. Chen, Y.-M. Wu, and Q.-G. Huang, Astrophys. J. **936**, 20 (2022).